A ACQUISITION FUNCTIONS α

$$\begin{aligned} \text{Variance Ratio} &= 1 - \frac{1}{T}\sum_{t=1}^{T}\left(\delta\left(\arg\max_c p(y=c|x,\omega_t) = \hat{c}\right)\right) \\ \hat{c} &= \arg\max_c \left(\arg\max_c p(y=c|x,\omega_t)\ \forall t \in (1,T)\right) \end{aligned} \tag{6}$$

where $\hat{c}$ is the most common class prediction across the T MC samples and δ is the Dirac delta function that evaluates to 1 if its argument is true, and 0 otherwise.

$$\text{Entropy H} = -\sum_{c=1}^{C} p(y=c|x)\log p(y=c|x) \tag{7}$$

$$\begin{aligned} \text{BALD} &= \text{JSD}(p_1, p_2, \ldots, p_T) \\ &= \text{H}(p(y|x)) - \mathbb{E}_{p(w|D_{train})}\left[\text{H}(p(y|x,w))\right] \end{aligned} \tag{8}$$

where C is the number of classes in the task formulation and $p(y=c|x,\omega)$ is the probability assigned by a network parameterised by ω to a particular class c when given an input x.

B Derivation of Monte Carlo Perturbations

$$\begin{aligned}\mathrm{BALD}_{\mathrm{MCP}} &= \mathrm{JSD}(p_1, p_2, \ldots, p_T) \\ &= \mathrm{H}(p(y|x)) - \mathbb{E}_{p(z|D_{train})}\left[\mathrm{H}(p(y|x,z))\right]\end{aligned} \tag{9}$$

$$\begin{aligned}\mathrm{H}(p(y|x)) &= \mathrm{H}\left(\int p(y|z)p(z|x)dz\right) \\ &= \mathrm{H}\left(\int p(y|z)q_\phi(z|x)dz\right) \\ &\approx \mathrm{H}\left(\frac{1}{T}\sum_{t=1}^{T} p(y|\hat{z}_t)\right)\end{aligned} \tag{10}$$

where z represents the perturbed input, T is the number of Monte Carlo samples, and $\hat{z}_t \sim q_\phi(z|x)$ is a sample from some perturbation generator.

$$\begin{aligned}\mathbb{E}_{p(z|D_{train})}\left[\mathrm{H}(p(y|x,z))\right] &= \mathbb{E}_{q_\phi(z|x)}\left[\mathrm{H}(p(y|x,z))\right] \\ &\approx \frac{1}{T}\sum_{t=1}^{T}\left[\mathrm{H}(p(y|\hat{z}_t))\right] \\ &= \frac{1}{T}\sum_{t=1}^{T}\left[-\sum_{c=1}^{C} p(y=c|\hat{z}_t)\log p(y=c|\hat{z}_t)\right]\end{aligned} \tag{11}$$

C Derivation of Bayesian Active Learning by Consistency

$$\mathrm{BALC}_{\mathrm{JSD}} = \mathbb{E}_{p(\omega|D_{train})}\left[\mathcal{D}_{KL}(p(y|x,\omega) \parallel p(y|z,\omega))\right] - \mathcal{D}_{KL}(p(y|x) \parallel p(y|z)) \tag{12}$$

where z is the perturbed version of the input and $\mathcal{D}_{KL}$ is the Kullback-Leibler divergence.

$$\begin{aligned}\mathbb{E}_{p(\omega|D_{train})}\left[\mathcal{D}_{KL}(p(y|x,\omega) \parallel p(y|z,\omega))\right] &= \mathbb{E}_{q_\theta(\omega)}\left[\mathcal{D}_{KL}(p(y|x,\omega) \parallel p(y|z,\omega))\right] \\ &\approx \frac{1}{T}\sum_{t=1}^{T}\left[\mathcal{D}_{KL}(p(y|x,\hat{\omega}_t \parallel p(y|\hat{x},\hat{\omega}_t))\right] \\ &= \frac{1}{T}\sum_{t=1}^{T}\left[\sum_{c=1}^{C} p(y=c|x,\hat{\omega}_t)\log\frac{p(y=c|x,\hat{\omega}_t)}{p(y=c|z,\hat{\omega}_t)}\right]\end{aligned} \tag{13}$$

$$\begin{aligned}\mathcal{D}_{KL}(p(y|x)||p(y|z)) &= \mathcal{D}_{KL}\left(\int p(y|\omega,x)p(\omega)d\omega \,\middle\|\, \int p(y|\omega,z)p(\omega)d\omega\right) \\ &= \mathcal{D}_{KL}\left(\int p(y|\omega,x)q_\theta(\omega)d\omega \,\middle\|\, \int p(y|\omega,z)q_\theta(\omega)d\omega\right) \\ &\approx \mathcal{D}_{KL}\left(\frac{1}{T}\sum_{t=1}^{T} p(y|\hat{\omega}_t,x) \,\middle\|\, \frac{1}{T}\sum_{t=1}^{T} p(y|\hat{\omega}_t,z)\right) \\ &= \frac{1}{C}\sum_{c=1}^{C}\left[\frac{1}{T}\sum_{t=1}^{T} p(y=c|\hat{\omega}_t,x)\log\frac{\frac{1}{T}\sum_{t=1}^{T} p(y=c|\hat{\omega}_t,x)}{\frac{1}{T}\sum_{t=1}^{T} p(y=c|\hat{\omega}_t,\hat{x})}\right]\end{aligned} \tag{14}$$

where the integral is approximated by T Monte Carlo samples, $\hat{\omega} \sim q_\theta(w)$ represents the parameters sampled from the Monte Carlo distribution, and C represents the number of classes in the task formulation.

D CHERNOFF BOUND ON ERROR RATE OF SELECTION NETWORK

D.1 DERIVATION OF CHERNOFF BOUND

In this section, we derive the Chernoff bound as an upper bound on the binary classification error, $P(\text{error})$, of the oracle selection network h_θ. This helps determine how reliable the output of h_θ is as a proxy for the classification performance of the main task.

$$
\begin{aligned}
P(\text{error}) &= \int_{-\infty}^{\infty} P(\text{error}|x)p(x)dx \\
&= \int_{-\infty}^{\infty} \min\left[P(y=0|x), P(y=1|x)\right] p(x)dx \\
&\leq \int_{-\infty}^{\infty} P(y=0|x)^{\beta} P(y=1|x)^{1-\beta} p(x)dx \\
&= P(y=0)^{\beta} P(y=1)^{1-\beta} \int_{-\infty}^{\infty} P(x|y=0)^{\beta} P(x|y=1)^{1-\beta} dx \\
&= P(y=0)^{\beta^*} P(y=1)^{1-\beta^*} e^{-\left[\frac{\beta^*(1-\beta^*)(\mu_0-\mu_1)^2}{2(\beta^*\sigma_0^2+(1-\beta^*)\sigma_1^2)} + \frac{1}{2} log \frac{\beta^*\sigma_0^2+(1-\beta^*)\sigma_1^2}{\sigma_0^{2\beta^*}\sigma_1^{2(1-\beta^*)}}\right]}
\end{aligned}
\tag{15}
$$

In order to calculate β^*, we minimize the following term using the Broyden-Fletcher-Goldfarb-Shannon (BFGS) algorithm with an initial value of $\beta_0 = 0$.

$$
\beta^* = \text{argmin}_\beta - \left[\frac{\beta(1-\beta)(\mu_0-\mu_1)^2}{2(\beta\sigma_0^2+(1-\beta)\sigma_1^2)} + \frac{1}{2} ln \frac{\beta\sigma_0^2+(1-\beta)\sigma_1^2}{\sigma_0^{2\beta}\sigma_1^{2(1-\beta)}}\right] \tag{16}
$$

E ALGORITHMS

E.1 BAYESIAN ACTIVE LEARNING BY CONSISTENCY

Algorithm 1 illustrates the BALC procedure with the option of incorporating temporal information shown in blue.

Algorithm 1: Bayesian Active Learning by Consistency

Input: acquisition epochs τ, temporal period Δt, labelled data $\mathcal{L}$, unlabelled data $\mathcal{U}$, network parameters ω, MC samples T, acquisition percentage b
while training **do**
  if epoch in Δt **then**
    for $x \sim \mathcal{U}$ **do**
      $z = x + \epsilon, \quad \epsilon \sim \mathcal{N}(0, \sigma^2)$
      for MC sample in T **do**
        obtain $p(y|x, \omega)$
        obtain $p(y|z, \omega)$
      end for
      calculate α using eq. 2 or eq. 1
      $\alpha(t) = \alpha$
    end for
  end if
  if epoch in τ **then**
    calculate α using eq. 3
    SortDescending(α)
    $\mathcal{U}_b \subseteq \mathcal{U}$
    $\mathcal{U} \in (\mathcal{U} \setminus \mathcal{U}_b)$
    $\mathcal{L} \in (\mathcal{L} \cup \mathcal{U}_b)$
  end if
end while

E.2 SOQAL

In this section, we outline the algorithm for performing SoQal. More specifically, Algorithm 2 presents the generic framework for the active learning procedure. Algorithm 3 elucidates the exact steps required to perform selective oracle questioning using SoQal.

Algorithm 2: Active Learning Procedure

Input: acquisition epochs τ, temporal period Δt, labelled data $\mathcal{L}$, unlabelled data $\mathcal{U}$, network parameters ω, MC samples T, acquisition percentage b
while training **do**
  if epoch in Δt **then**
    for $x \sim \mathcal{U}$ **do**
      for MC sample in T **do**
        obtain $p(y|x, \omega)$
      end for
      calculate α
    end for
  end if
  if epoch in τ **then**
    SortDescending(α)
    $x_b \subset X_U$
    $y_b = \text{SoQal}(x_b)$
    $\mathcal{U} \in (\mathcal{U} \setminus (x_b, y_b))$
    $\mathcal{L} \in (\mathcal{L} \cup (x_b, y_b))$
  end if
end while

Algorithm 3: SoQal

Input: unlabelled inputs x_b, Hellinger distance $\mathcal{D}_H$, Hellinger threshold S
for $x \sim x_b$ **do**
  $o = g_\theta(x)$
  if $\mathcal{D}_H > S$ **then**
    calculate p(asking oracle) from eq. 5
    if p(asking oracle) $= 1$ **then**
      $y_b \subset Y_U$
    else
      $y_b = \text{argmax} p(y|x, \omega)$
    end if
  end if
end for

F DATASETS

F.1 DATA PREPROCESSING

Each dataset consists of cardiac time-series waveforms alongside their corresponding cardiac arrhythmia label. Each waveform was split into non-overlapping frames of 2500 samples.

PhysioNet 2015 PPG, $\mathcal{D}_1$ (Clifford et al., 2015). This dataset consists of photoplethysmogram (PPG) time-series waveforms sampled at 250Hz and five cardiac arrhythmia labels: Asystole, Extreme Bradycardia, Extreme Tachycardia, Ventricular Tachycardia, and Ventricular Fibrillation. Only patients with a True Positive Alarm are considered. The PPG frames were normalized in amplitude between the values of 0 and 1.

PhysioNet 2015 ECG, $\mathcal{D}_2$ (Clifford et al., 2015). This dataset consists of electrocardiogram (ECG) time-series waveforms sampled at 250Hz and five cardiac arrhythmia labels: Asystole, Extreme Bradycardia, Extreme Tachycardia, Ventricular Tachycardia, and Ventricular Fibrillation. Only patients with a True Positive Alarm are considered. The ECG frames were normalized in amplitude between the values of 0 and 1.

PhysioNet 2017 ECG, $\mathcal{D}_3$ (Clifford et al., 2017). This dataset consists of ECG time-series waveforms sampled at 300Hz and four labels: Normal, Atrial Fibrillation, Other, and Noisy. The ECG frames were not normalized.

Cardiology ECG, $\mathcal{D}_4$ (Hannun et al., 2019). This dataset consists of ECG time-series waveforms sampled at 200Hz and twelve cardiac arrhythmia labels: Atrial Fibrillation, Atrio-ventricular Block, Bigeminy, Ectopic Atrial Rhythm, Idioventricular Rhythm, Junctional Rhythm, Noise, Sinus Rhythm, Supraventricular Tachycardia, Trigeminy, Ventricular Tachycardia, and Wenckebach. Sudden bradycardia cases were excluded from the data as they were not included in the original formulation by the authors. The ECG frames were not normalized.

CIFAR10, $\mathcal{D}_5$ (Krizhevsky et al., 2009). This dataset consists of 60,000 colour images of dimension 32×32 associated with 10 classes. These classes are $\mathrm{airplane}$, $\mathrm{automobile}$, bird, cat, deer, dog, frog, horse, ship, and truck. Each image was normalized between the range of -1 and 1. No data augmentation was applied during the training procedure.

F.2 DATA SAMPLES

All datasets were split into training, validation, and test sets according to patient ID using a 60, 20, 20 configuration. In other words, patients appeared in only one of the sets. Samples in the training set were further split into a labelled and an unlabelled subset, also according to patient ID. In Tables 2 and 3, we show the number of samples and patients used in each of these sets.

F.2.1 CONSISTENCY-BASED ACTIVE LEARNING EXPERIMENTS

Table 2: Sample sizes (number of patients for cardiac datasets) of train/val/test splits. Datasets $\mathcal{D}_1$ to $\mathcal{D}_4$ are defined in Sec. 5.1 of the main manuscript.

Dataset	Fraction β	Train Labelled	Train Unlabelled	Val	Test
$\mathcal{D}_1$	0.1	401 (18)	4,233 (171)	1,124 (47)	1,435 (58)
	0.3	1,285 (55)	3,349 (134)		
	0.5	2,187 (92)	2,447 (97)		
	0.7	3,132 (129)	1,502 (60)		
	0.9	4,184 (166)	450 (23)		
$\mathcal{D}_2$	0.1	401 (18)	4,233 (171)	1,124 (47)	1,435 (58)
	0.3	1,285 (55)	3,349 (134)		
	0.5	2,187 (92)	2,447 (97)		
	0.7	3,132 (129)	1,502 (60)		
	0.9	4,184 (166)	450 (23)		
$\mathcal{D}_3$	0.1	1,776 (545)	16,479 (4,914)	4,582 (1,364)	5,824 (1705)
	0.3	5,399 (1636)	12,856 (3,823)		
	0.5	9,054 (2727)	9,201 (2,732)		
	0.7	12,733 (3818)	5,522 (1,641)		
	0.9	16,365 (4909)	1,890 (550)		
$\mathcal{D}_4$	0.1	452 (20)	4,110 (181)	1,131 (50)	1,386 (62)
	0.3	1,368 (60)	3,194 (141)		
	0.5	2,280 (101)	2,282 (100)		
	0.7	3,200 (140)	1,362 (61)		
	0.9	4,079 (180)	483 (21)		
$\mathcal{D}_5$	0.5	20,000	20,000	10,000	10,000
	0.7	28,000	12,000		
	0.9	36,000	4,000		

F.2.2 SELECTIVE ORACLE QUESTIONING EXPERIMENTS

Table 3: Sample sizes (number of patients) of training, validation, and test sets.

Dataset	Training Labelled	Training Unlabelled	Validation	Test
$\mathcal{D}_1$	401 (18)	4233 (171)	1124 (47)	1435 (58)
$\mathcal{D}_2$	401 (18)	4233 (171)	1124 (47)	1435 (58)
$\mathcal{D}_3$	1,776 (545)	16,479 (4,914)	4,582 (1,364)	5,824 (1,705)
$\mathcal{D}_4$	452 (20)	4,110 (181)	1,131 (50)	1,386 (62)
$\mathcal{D}_5$	676 (12)	5,880 (116)	1,566 (32)	1,971 (40)

G IMPLEMENTATION DETAILS

In this section, we outline the network architecture used for all experiments conducted in the main manuscript. We also outline the batchsize and learning rate associated with training on each of the datasets.

G.1 NETWORK ARCHITECTURE

Table 4: Network architectures used for time-series and image experiments. K, C_{in}, and C_{out} represent the kernel size, number of input channels, and number of output channels, respectively. A stride of 3 and 1 was used for Conv1D and Conv2D operators, respectively.

(a) Network for time-series datasets

Layer Number	Layer Components	Kernel Dimension
1	Conv 1D BatchNorm ReLU MaxPool(2) Dropout(0.1)	7 x 1 x 4 (K x C_{in} x C_{out})
2	Conv 1D BatchNorm ReLU MaxPool(2) Dropout(0.1)	7 x 4 x 16
3	Conv 1D BatchNorm ReLU MaxPool(2) Dropout(0.1)	7 x 16 x 32
4	Linear ReLU	320 x 100
5	Linear	100 x C (classes)

(b) Network for CIFAR10

Layer Number	Layer Components	Kernel Dimension
1	Conv 2D ReLU MaxPool(2)	5 x 3 x 6
2	Conv 2D ReLU MaxPool(2)	5 x 6 x 16
3	Linear ReLU Dropout(0.1)	160 x 120
4	Linear ReLU Dropout(0.1)	120 x 84
5	Linear	84 x C (classes)

G.2 EXPERIMENT DETAILS

Table 5: Batchsize and learning rates used for training with different datasets. The Adam optimizer was used for all experiments.

Dataset	Batchsize	Learning Rate
$\mathcal{D}_1$	256	10^{-4}
$\mathcal{D}_2$	256	10^{-4}
$\mathcal{D}_3$	256	10^{-4}
$\mathcal{D}_4$	16	10^{-4}

G.3 PERTURBATION DETAILS

When conducting the MCP and BALC experiments, we perturbed each of the time-series frames with additive Gaussian noise, $\epsilon \sim \mathcal{N}(0, \sigma)$ where we chose σ based on the specific dataset to avoid introducing too much noise. For CIFAR10, we perturbed the images by applying a sequence of data augmentation steps inspired by work in Chen et al. (2020). The details of these perturbations can be found in Table 6. We applied all perturbations to the input data before normalization.

Table 6: Perturbations applied to different datasets during MCP and BALC implementations. p represents the probability of applying a particular augmentation method.

Dataset	Perturbation
$\mathcal{D}_1$	$\epsilon \sim \mathcal{N}(0, 100)$
$\mathcal{D}_2$	$\epsilon \sim \mathcal{N}(0, 100)$
$\mathcal{D}_3$	$\epsilon \sim \mathcal{N}(0, 100)$
$\mathcal{D}_4$	$\epsilon \sim \mathcal{N}(0, 100)$
$\mathcal{D}_5$	1) $\mathrm{RandomResizedCrop}(\mathrm{scale} = (0.8, 1.0))$ 2) $\mathrm{RandomApply}(\mathrm{ColorJitter}(0.8,0.8,0.8,0.2), p = 0.2)$ 3) $\mathrm{RandomGrayscale}(p = 0.2)$

G.4 BASELINE IMPLEMENTATIONS

In this section, we outline our implementation of the baseline methods used in the selective oracle questioning experiments.

G.4.1 ENTROPY RESPONSE

This approach is anchored around the idea that network outputs that exhibit high entropy (i.e., close to a uniform distribution) are likely to correspond to instances that the network is uncertain of. Consequently, we exploited this idea to determine whether a label is requested from an oracle or if a pseudo-label should be generated instead. More specifically, we introduced a threshold, $\mathrm{S}_{Entropy} = w \times \mathrm{S}_{Max}$, which is a fraction of the maximum entropy possible for a particular classification problem. As mentioned, $\mathrm{S}_{Max} = \log C$, where C is the number of classes. We chose $w = 0.9$ to balance between oracle dependence and pseudo-label accuracy. This value was kept fixed during training. In our implementation, we take the mean of the network outputs as a result of the perturbations, calculate its entropy, and determine whether it exceeds the aforementioned threshold. If it does, then the uncertainty is deemed high and a label is requested from an oracle.

G.4.2 EPSILON GREEDY

This approach is inspired by the reinforcement learning literature and is used to decay the dependence of network on the oracle. More specifically, we define $\epsilon = e^{\frac{-\text{epoch}}{k \times \tau}}$ where epoch represents the training epoch number and τ is the epoch interval at which acquisitions are performed. ϵ decays from $1 \rightarrow 0$ as training progresses. We chose $k = \tau = 5$ in order to balance between oracle dependence and pseudo-label accuracy. To determine whether a label is requested from an oracle, we generate a random number, $R \sim \mathcal{U}(0, 1)$, for a uniform distribution and check whether it is below ϵ. If this is satisfied, then an oracle is requested for a label, and a pseudo-label is generated otherwise. As designed, this approach starts off with 100% dependence on an oracle and decays towards minimal dependence as training progresses.

H TEST SET PERFORMANCE IN THE ABSENCE OF ORACLE

In this section, we quantify and compare the performance of our consistency-based active learning framework to state-of-the-art AL methods on four diverse datasets, $\mathcal{D}_1$ - $\mathcal{D}_4$ and for a range of fraction values, $\beta = (0.1, 0.3, 0.5, 0.7, 0.9)$. Across Tables 7 - 11, we show that our method outperforms the baseline methods in 17 out of 28 (61%) experimental categories. Moreover, in half of all experimental categories, temporal acquisition functions perform best.

H.1 PHYSIONET 2015 PPG, $\mathcal{D}_1$

Table 7: Mean test Set AUC on $\mathcal{D}_1$. Bolded elements represent the best performing method and acquisition function α for each fraction β. No AL represents training without an active learning strategy. Results shown across 5 seeds.

Fraction β	Method	Acquisition Metric								No AL
		Non-temporal				Temporal				
		Var Ratio	Entropy	BALD	-	Var Ratio	Entropy	BALD	-	
0.1	MCD	0.476 ± 0.022	0.475 ± 0.020	0.465 ± 0.017	-	0.468 ± 0.032	0.492 ± 0.022	0.476 ± 0.015	-	0.577 ± 0.014
	MCP	0.475 ± 0.037	0.448 ± 0.019	0.464 ± 0.023	-	0.497 ± 0.028	0.490 ± 0.032	$\mathbf{0.515 \pm 0.025}$	-	
	BALC_{JSD}	-	-	-	0.511 ± 0.031	-	-	-	0.494 ± 0.021	
	BALC_{KLD}	-	-	-	0.500 ± 0.023	-	-	-	0.496 ± 0.024	
0.3	MCD	0.603 ± 0.021	0.618 ± 0.026	0.606 ± 0.032	-	0.607 ± 0.012	0.614 ± 0.009	0.617 ± 0.035	-	0.653 ± 0.017
	MCP	0.633 ± 0.024	0.607 ± 0.015	0.598 ± 0.015	-	0.626 ± 0.032	0.627 ± 0.026	0.606 ± 0.031	-	
	BALC_{JSD}	-	-	-	0.594 ± 0.009	-	-	-	0.600 ± 0.016	
	BALC_{KLD}	-	-	-	$\mathbf{0.633 \pm 0.017}$	-	-	-	0.617 ± 0.019	
0.5	MCD	0.650 ± 0.011	0.650 ± 0.011	0.660 ± 0.013	-	0.654 ± 0.014	0.653 ± 0.024	0.655 ± 0.008	-	0.665 ± 0.007
	MCP	0.655 ± 0.013	0.653 ± 0.008	0.647 ± 0.019	-	0.642 ± 0.027	$\mathbf{0.669 \pm 0.016}$	0.648 ± 0.012	-	
	BALC_{JSD}	-	-	-	0.658 ± 0.003	-	-	-	0.652 ± 0.025	
	BALC_{KLD}	-	-	-	0.662 ± 0.015	-	-	-	0.661 ± 0.014	
0.7	MCD	0.650 ± 0.008	0.640 ± 0.008	$\mathbf{0.658 \pm 0.010}$	-	0.656 ± 0.008	0.636 ± 0.0134	0.655 ± 0.007	-	0.642 ± 0.015
	MCP	0.653 ± 0.010	0.652 ± 0.009	0.654 ± 0.008	0.646 ± 0.015	-	0.649 ± 0.006	0.651 ± 0.010	-	
	BALC_{JSD}	-	-	-	0.642 ± 0.011	-	-	-	0.649 ± 0.008	
	BALC_{KLD}	-	-	-	0.653 ± 0.010	-	-	-	0.656 ± 0.012	
0.9	MCD	$\mathbf{0.704 \pm 0.009}$	0.691 ± 0.012	0.698 ± 0.018	-	0.690 ± 0.022	0.693 ± 0.015	0.692 ± 0.020	-	0.680 ± 0.039
	MCP	0.702 ± 0.019	0.678 ± 0.020	0.700 ± 0.015	-	0.703 ± 0.016	0.680 ± 0.017	0.692 ± 0.009	-	
	BALC_{JSD}	-	-	-	0.690 ± 0.006	-	-	-	0.700 ± 0.028	
	BALC_{KLD}	-	-	-	0.699 ± 0.011	-	-	-	0.689 ± 0.013	

H.2 PHYSIONET 2015 ECG, $\mathcal{D}_2$

Table 8: Test Set AUC on $\mathcal{D}_2$. Bolded elements represent the best performing method and acquisition function α for each fraction β. No AL represents training without an active learning strategy. Results are averaged across 5 seeds.

Fraction β	Method	Acquisition Metric								No AL
		Non-temporal				Temporal				
		Var Ratio	Entropy	BALD	-	Var Ratio	Entropy	BALD	-	
0.1	MCD	0.567 ± 0.029	0.591 ± 0.040	0.573 ± 0.063	-	0.547 ± 0.058	0.584 ± 0.055	0.598 ± 0.050	-	0.679 ± 0.040
	MCP	0.567 ± 0.027	0.557 ± 0.032	0.589 ± 0.045	-	0.548 ± 0.036	0.549 ± 0.046	0.554 ± 0.055	-	
	BALC_{JSD}	-	-	-	0.576 ± 0.050	-	-	-	0.574 ± 0.057	
	BALC_{KLD}	-	-	-	$\mathbf{0.602 \pm 0.044}$	-	-	-	0.575 ± 0.017	
0.3	MCD	0.675 ± 0.022	0.666 ± 0.053	0.643 ± 0.036	-	0.644 ± 0.019	$\mathbf{0.692 \pm 0.020}$	0.684 ± 0.035	-	0.605 ± 0.020
	MCP	0.678 ± 0.036	0.660 ± 0.071	0.665 ± 0.051	-	0.643 ± 0.038	0.668 ± 0.020	0.658 ± 0.026	-	
	BALC_{JSD}	-	-	-	0.654 ± 0.033	-	-	-	0.677 ± 0.032	
	BALC_{KLD}	-	-	-	0.634 ± 0.032	-	-	-	0.672 ± 0.049	
0.5	MCD	0.676 ± 0.0434	0.700 ± 0.031	0.668 ± 0.0185	-	0.709 ± 0.0407	0.694 ± 0.0431	0.669 ± 0.0238	-	0.703 ± 0.032
	MCP	0.687 ± 0.0183	0.695 ± 0.0212	0.712 ± 0.0235	-	0.700 ± 0.0135	0.709 ± 0.0261	0.680 ± 0.0247	-	
	BALC_{JSD}	-	-	-	0.701 ± 0.026	-	-	-	0.703 ± 0.018	
	BALC_{KLD}	-	-	-	0.705 ± 0.045	-	-	-	$\mathbf{0.726 \pm 0.031}$	
0.7	MCD	0.758 ± 0.016	0.765 ± 0.027	0.754 ± 0.014	-	0.753 ± 0.020	0.766 ± 0.025	0.755 ± 0.024	-	0.747 ± 0.010
	MCP	0.744 ± 0.031	0.759 ± 0.022	0.745 ± 0.027	-	0.757 ± 0.013	$\mathbf{0.777 \pm 0.025}$	0.764 ± 0.014	-	
	BALC_{JSD}	-	-	-	0.750 ± 0.006	-	-	-	0.746 ± 0.016	
	BALC_{KLD}	-	-	-	0.730 ± 0.035	-	-	-	0.761 ± 0.028	
0.9	MCD	0.742 ± 0.016	0.745 ± 0.048	0.757 ± 0.015	-	0.769 ± 0.0261	0.766 ± 0.018	0.754 ± 0.015	-	0.747 ± 0.011
	MCP	0.765 ± 0.013	0.759 ± 0.028	0.751 ± 0.013	-	0.758 ± 0.018	0.759 ± 0.021	0.743 ± 0.025	-	
	BALC_{JSD}	-	-	-	0.726 ± 0.008	-	-	-	$\mathbf{0.771 \pm 0.018}$	
	BALC_{KLD}	-	-	-	0.762 ± 0.037	-	-	-	0.749 ± 0.020	

H.3 PHYSIONET 2017 ECG, $\mathcal{D}_3$

Table 9: Test Set AUC on $\mathcal{D}_3$. Bolded elements represent the best performing method and acquisition function α for each fraction β. No AL represents training without an active learning strategy. Results are averaged across 5 seeds.

Fraction β	Method	Acquisition Metric								No AL
		Non-temporal				Temporal				
		Var Ratio	Entropy	BALD	-	Var Ratio	Entropy	BALD	-	
0.1	MCD	0.628 ± 0.006	0.620 ± 0.006	0.581 ± 0.014	-	0.614 ± 0.03	0.610 ± 0.013	0.562 ± 0.019	-	0.716 ± 0.012
	MCP	0.624 ± 0.017	0.621 ± 0.018	0.623 ± 0.020	-	0.605 ± 0.027	0.613 ± 0.026	0.622 ± 0.026	-	
	BALC_{JSD}	-	-	-	0.613 ± 0.013	-	-	-	0.611 ± 0.015	
	BALC_{KLD}	-	-	-	$\mathbf{0.631 \pm 0.010}$	-	-	-	0.600 ± 0.005	
0.3	MCD	0.705 ± 0.003	0.672 ± 0.009	0.688 ± 0.011	-	0.704 ± 0.016	0.685 ± 0.010	0.684 ± 0.0081	-	0.766 ± 0.012
	MCP	0.688 ± 0.018	0.673 ± 0.007	$\mathbf{0.719 \pm 0.016}$	-	0.671 ± 0.016	0.684 ± 0.018	0.699 ± 0.023	-	
	BALC_{JSD}	-	-	-	0.694 ± 0.006	-	-	-	0.681 ± 0.010	
	BALC_{KLD}	-	-	-	0.703 ± 0.023	-	-	-	0.701 ± 0.015	
0.5	MCD	0.744 ± 0.013	0.735 ± 0.007	0.749 ± 0.012	-	$\mathbf{0.772 \pm 0.015}$	0.743 ± 0.018	0.758 ± 0.009	-	0.790 ± 0.012
	MCP	0.744 ± 0.008	0.733 ± 0.006	0.747 ± 0.004	-	0.741 ± 0.013	0.752 ± 0.019	0.732 ± 0.038	-	
	BALC_{JSD}	-	-	-	0.763 ± 0.022	-	-	-	0.771 ± 0.011	
	BALC_{KLD}	-	-	-	0.769 ± 0.006	-	-	-	0.761 ± 0.003	
0.7	MCD	0.802 ± 0.006	0.811 ± 0.007	0.809 ± 0.004	-	0.807 ± 0.010	0.807 ± 0.003	$\mathbf{0.815 \pm 0.010}$	-	0.810 ± 0.008
	MCP	0.786 ± 0.003	0.782 ± 0.011	0.784 ± 0.016	-	0.772 ± 0.014	0.765 ± 0.013	0.762 ± 0.018	-	
	BALC_{JSD}	-	-	-	0.803 ± 0.011	-	-	-	0.813 ± 0.010	
	BALC_{KLD}	-	-	-	0.809 ± 0.006	-	-	-	0.810 ± 0.005	
0.9	MCD	0.820 ± 0.006	0.824 ± 0.005	0.828 ± 0.004	-	0.821 ± 0.011	0.823 ± 0.005	0.825 ± 0.006	-	0.827 ± 0.004
	MCP	0.826 ± 0.002	0.821 ± 0.007	0.807 ± 0.011	-	0.828 ± 0.008	0.812 ± 0.009	0.808 ± 0.012	-	
	BALC_{JSD}	-	-	-	0.825 ± 0.003	-	-	-	0.824 ± 0.011	
	BALC_{KLD}	-	-	-	0.827 ± 0.005	-	-	-	$\mathbf{0.829 \pm 0.007}$	

H.4 CARDIOLOGY ECG, $\mathcal{D}_4$

Table 10: Test Set AUC on $\mathcal{D}_4$. Bolded elements represent the best performing method and acquisition function α for each fraction β. No AL represents training without an active learning strategy. Results are averaged across 5 seeds.

Fraction β	Method	Acquisition Metric								No AL
		Non-temporal				Temporal				
		Var Ratio	Entropy	BALD	-	Var Ratio	Entropy	BALD	-	
0.1	MCD	0.475 ± 0.039	$\mathbf{0.518 \pm 0.016}$	0.486 ± 0.011	-	0.485 ± 0.029	0.491 ± 0.022	0.484 ± 0.040	-	0.486 ± 0.023
	MCP	0.508 ± 0.031	0.492 ± 0.022	0.493 ± 0.030	-	0.500 ± 0.024	0.478 ± 0.024	0.492 ± 0.022	-	
	BALC_{JSD}	-	-	-	0.460 ± 0.043	-	-	-	0.487 ± 0.042	
	BALC_{KLD}	-	-	-	0.505 ± 0.032	-	-	-	0.511 ± 0.030	
0.3	MCD	0.487 ± 0.012	0.510 ± 0.018	0.498 ± 0.026	-	0.491 ± 0.014	0.496 ± 0.015	0.500 ± 0.025	-	0.533 ± 0.020
	MCP	0.520 ± 0.007	0.480 ± 0.019	0.494 ± 0.019	-	0.497 ± 0.007	$\mathbf{0.529 \pm 0.035}$	0.498 ± 0.021	-	
	BALC_{JSD}	-	-	-	0.488 ± 0.025	-	-	-	0.487 ± 0.016	
	BALC_{KLD}	-	-	-	0.510 ± 0.030	-	-	-	0.494 ± 0.014	
0.5	MCD	0.563 ± 0.021	$\mathbf{0.591 \pm 0.008}$	0.562 ± 0.011	-	0.557 ± 0.025	0.580 ± 0.006	0.569 ± 0.010	-	0.581 ± 0.019
	MCP	0.529 ± 0.027	0.554 ± 0.024	0.544 ± 0.015	-	0.557 ± 0.021	0.536 ± 0.013	0.526 ± 0.012	-	
	BALC_{JSD}	-	-	-	0.559 ± 0.001	-	-	-	0.559 ± 0.003	
	BALC_{KLD}	-	-	-	0.575 ± 0.028	-	-	-	0.576 ± 0.011	
0.7	MCD	0.637 ± 0.010	0.615 ± 0.010	0.639 ± 0.016	-	0.633 ± 0.016	0.652 ± 0.028	0.662 ± 0.014	-	0.630 ± 0.008
	MCP	0.626 ± 0.018	0.626 ± 0.013	0.623 ± 0.031	-	0.623 ± 0.012	0.623 ± 0.003	0.624 ± 0.010	-	
	BALC_{JSD}	-	-	-	0.634 ± 0.024	-	-	-	$\mathbf{0.648 \pm 0.023}$	
	BALC_{KLD}	-	-	-	0.625 ± 0.015	-	-	-	0.632 ± 0.028	
0.9	MCD	0.651 ± 0.008	0.666 ± 0.011	0.666 ± 0.017	-	0.670 ± 0.007	0.653 ± 0.025	$\mathbf{0.677 \pm 0.009}$	-	0.660 ± 0.013
	MCP	0.655 ± 0.027	0.673 ± 0.009	0.672 ± 0.017	-	0.663 ± 0.006	0.662 ± 0.005	0.670 ± 0.009	-	
	BALC_{JSD}	-	-	-	0.656 ± 0.015	-	-	-	0.656 ± 0.019	
	BALC_{KLD}	-	-	-	0.666 ± 0.025	-	-	-	0.663 ± 0.013	

H.5 CIFAR10, $\mathcal{D}_5$

Table 11: Test Set Accuracy on $\mathcal{D}_5$. Bolded elements represent the best performing method and acquisition function α for each fraction β. No AL represents training without an active learning strategy. Results are averaged across 5 seeds.

Fraction β	Method	Acquisition Metric								No AL
		Non-temporal				Temporal				
		Var Ratio	Entropy	BALD	-	Var Ratio	Entropy	BALD	-	
0.5	MCD	0.566 ± 0.012	0.565 ± 0.010	0.558 ± 0.008	-	0.565 ± 0.008	0.559 ± 0.010	0.562 ± 0.007	-	0.576 ± 0.008
	MCP	0.553 ± 0.009	0.562 ± 0.009	0.561 ± 0.004	-	$\mathbf{0.569 \pm 0.004}$	0.562 ± 0.012	0.554 ± 0.009	-	
	BALC_{JSD}	-	-	-	0.552 ± 0.009	-	-	-	0.565 ± 0.012	
	BALC_{KLD}	-	-	-	0.564 ± 0.010	-	-	-	0.566 ± 0.008	
0.7	MCD	0.586 ± 0.009	0.590 ± 0.009	0.597 ± 0.009	-	0.588 ± 0.006	0.593 ± 0.008	0.594 ± 0.003	-	0.593 ± 0.011
	MCP	$\mathbf{0.600 \pm 0.002}$	0.589 ± 0.010	0.585 ± 0.005	-	0.595 ± 0.010	0.592 ± 0.009	0.599 ± 0.002	-	
	BALC_{JSD}	-	-	-	0.600 ± 0.006	-	-	-	0.589 ± 0.008	
	BALC_{KLD}	-	-	-	0.594 ± 0.007	-	-	-	0.596 ± 0.013	
0.9	MCD	0.618 ± 0.004	0.612 ± 0.007	0.618 ± 0.008	-	0.610 ± 0.004	0.616 ± 0.004	0.615 ± 0.007	-	0.608 ± 0.012
	MCP	0.610 ± 0.002	0.612 ± 0.007	0.610 ± 0.011	-	0.612 ± 0.010	$\mathbf{0.621 \pm 0.004}$	0.608 ± 0.015	-	
	BALC_{JSD}	-	-	-	0.613 ± 0.006	-	-	-	0.609 ± 0.006	
	BALC_{KLD}	-	-	-	0.618 ± 0.010	-	-	-	0.612 ± 0.007	

I BASELINE VALIDATION PERFORMANCE AS A FUNCTION OF FRACTION LEVEL, β

The availability of labelled training data is known to affect network performance. To quantify this effect, we illustrate, in Fig. 7, the validation AUC (Accuracy for $\mathcal{D}_5$) for a range of fractions $\beta = (0.1, 0.3, 0.5, 0.7, 0.9)$. As expected, we observe a graded response where the larger the amount of labelled training data, the better the generalization performance of the network. This can be seen by the higher AUC achieved when using $\beta = 0.9$ compared to when using $\beta = 0.1$.

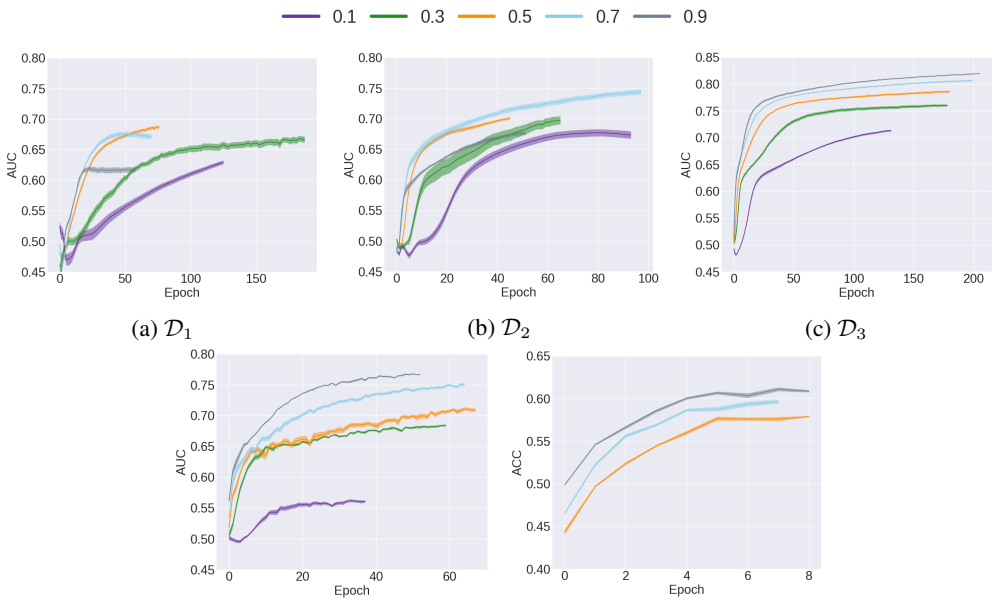

(a) $\mathcal{D}_1$ (b) $\mathcal{D}_2$ (c) $\mathcal{D}_3$

(d) $\mathcal{D}_4$ (e) $\mathcal{D}_5$

Figure 7: Baseline validation AUC for $\mathcal{D}_1$ - $\mathcal{D}_4$ and Accuracy for $\mathcal{D}_5$ at different fraction levels β. These represent the performance curves for the training procedure without active learning. As β increases, performance typically improves.

J VALIDATION SET AUC WITH NON-TEMPORAL ACQUISITION FUNCTIONS IN THE ABSENCE OF ORACLE

In the main manuscript, we presented a subset of results for experiments in which oracles are absent and thus unavailable to provide annotations. Instead, unlabelled instances are pseudo-labelled based on network-generated predictions. In this section, we include an exhaustive set of results for all those experiments. More specifically, we illustrate in Figs. 8 - 12 the validation AUC of the various AL methods for datasets $\mathcal{D}_1$ - $\mathcal{D}_5$. At a high level and across datasets, we find that the cold-start problem is likely to occur at low fraction values ($\beta = 0.1$). We include more details in the respective sections.

J.1 PHYSIONET 2015 PPG, $\mathcal{D}_1$

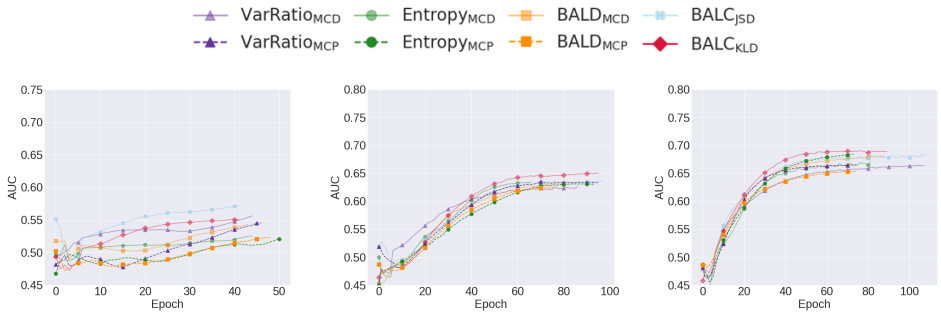

(a) $\beta = 0.1$ (b) $\beta = 0.3$ (c) $\beta = 0.5$

(d) $\beta = 0.7$ (e) $\beta = 0.9$

Figure 8: Mean validation set AUC for the various methodologies and acquisition functions on $\mathcal{D}_1$ at increasing fraction levels $\beta = (0.1, 0.3, 0.5, 0.7, 0.9)$. The no-oracle cold-start problem is observed at $\beta = 0.1$ where active learning approaches fail due to few available labelled training instances. Clear benefits of our methods can be seen at $\beta = 0.5, 0.7$. Results are averaged across 5 seeds.

J.2 PHYSIONET 2015 ECG, $\mathcal{D}_2$

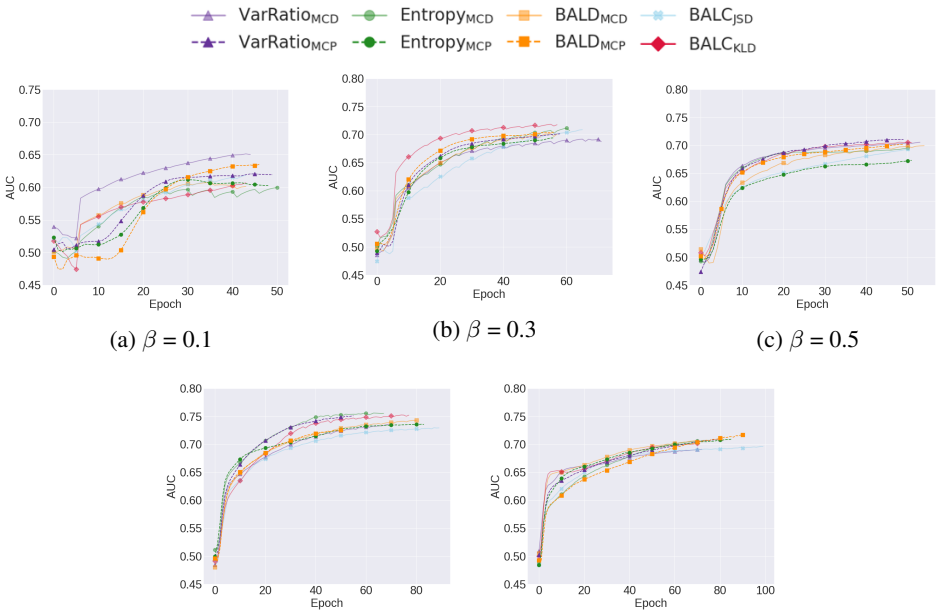

(a) $\beta = 0.1$ (b) $\beta = 0.3$ (c) $\beta = 0.5$

(d) $\beta = 0.7$ (e) $\beta = 0.9$

Figure 9: Mean validation set AUC for the various methodologies and acquisition functions on $\mathcal{D}_2$ at increasing fraction levels $\beta = (0.1, 0.3, 0.5, 0.7, 0.9)$. Our methods include MCP and BALC methods. The no-oracle cold-start problem is observed at $\beta = 0.1$ where active learning approaches fail due to few available labelled training instances. However, our approaches outperform all others at $\beta = 0.3, 0.5, 0.7, 0.9$. Results are averaged across 5 seeds.

J.3 PHYSIONET 2017 ECG, $\mathcal{D}_3$

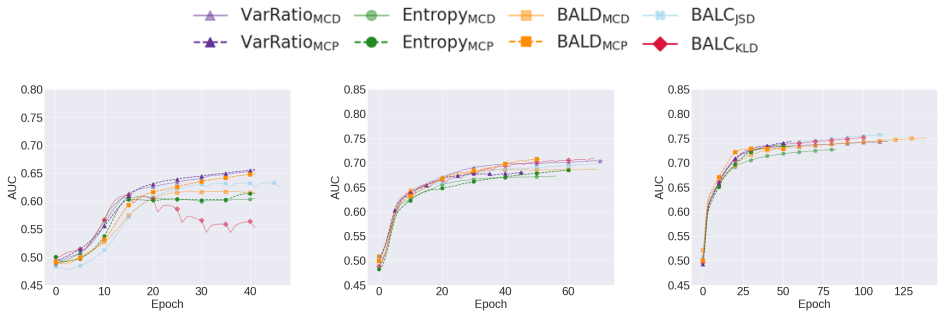

(a) $\beta = 0.1$ (b) $\beta = 0.3$ (c) $\beta = 0.5$

(d) $\beta = 0.7$ (e) $\beta = 0.9$

Figure 10: Mean validation set AUC for the various methodologies and acquisition functions on $\mathcal{D}_3$ at increasing fraction levels $\beta = (0.1, 0.3, 0.5, 0.7, 0.9)$. Our methods include MCP and BALC methods. The no-oracle cold-start problem is observed at $\beta = 0.1$ where active learning approaches fail due to few available labelled training instances. Most methods perform on par with the no active learning strategy for this particular dataset. Results are averaged across 5 seeds.

J.4 CARDIOLOGY ECG, $\mathcal{D}_4$

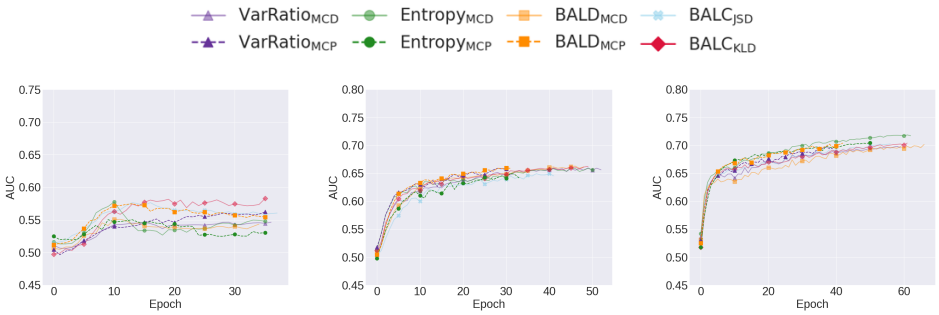

(a) $\beta = 0.1$ (b) $\beta = 0.3$ (c) $\beta = 0.5$

(d) $\beta = 0.7$ (e) $\beta = 0.9$

Figure 11: Mean validation set AUC for the various methodologies and acquisition functions on $\mathcal{D}_4$ at increasing fraction levels $\beta = (0.1, 0.3, 0.5, 0.7, 0.9)$. Our methods include MCP and BALC methods. The no-oracle cold-start problem is *not* observed for this dataset. Most methods perform comparably to one another at high values of β. Results are averaged across 5 seeds.

J.5 CIFAR10, $\mathcal{D}_5$

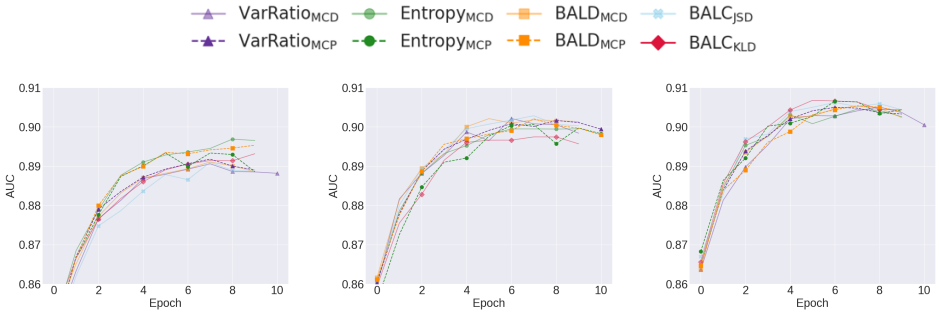

(a) $\beta = 0.5$ (b) $\beta = 0.7$ (c) $\beta = 0.9$

Figure 12: Mean validation set AUC for the various methodologies and acquisition functions on $\mathcal{D}_5$ at increasing fraction levels β = (0.5, 0.7, 0.9). Our methods include MCP and BALC methods. At all fractions, we show that MCP methods outperform their MCD counterparts. Results are averaged across 5 seeds.

K EFFECT OF MCP WITH TRACKED ACQUISITION FUNCTIONS ON PERFORMANCE

In this section, we are interested in quantifying the effect of implementing a temporal acquisition function in conjunction with MCP on performance. In Fig. 13, we illustrate two columns of matrices. The first column reflects the percent change in generalization performance between implementing MCP and MCD with static temporal functions (i.e., without tracking) for three different datasets. We find that there are mixed results. For example, on $mathcal D_2$ at $\beta = 0.5$, BALD_{MCP} outperforms BALD_{MCD} by 6.5%. However, on $mathcal D_4$ at $\beta = 0.5$, $\text{Entropy}_{\text{MCP}}$ performs worse than $\text{Entropy}_{\text{MCD}}$ by 6.7%. Furthermore, upon applying tracked acquisition functions, we also obtain mixed results. In many cases, there are notable improvements. For example, on $mathcal D_3$ at $\beta = 0.5$, $\text{Temporal Entropy}_{\text{MCP}}$ improves performance by an additional $0.3 + 2.3 = 2.6\%$. On the other hand, at $\beta = 0.7$, $\text{Temporal Entropy}_{\text{MCP}}$ worsens performance by 2.1%. Based on these findings, we would recommend that the utility of temporal acquisition functions be determined on a case-by-case basis.

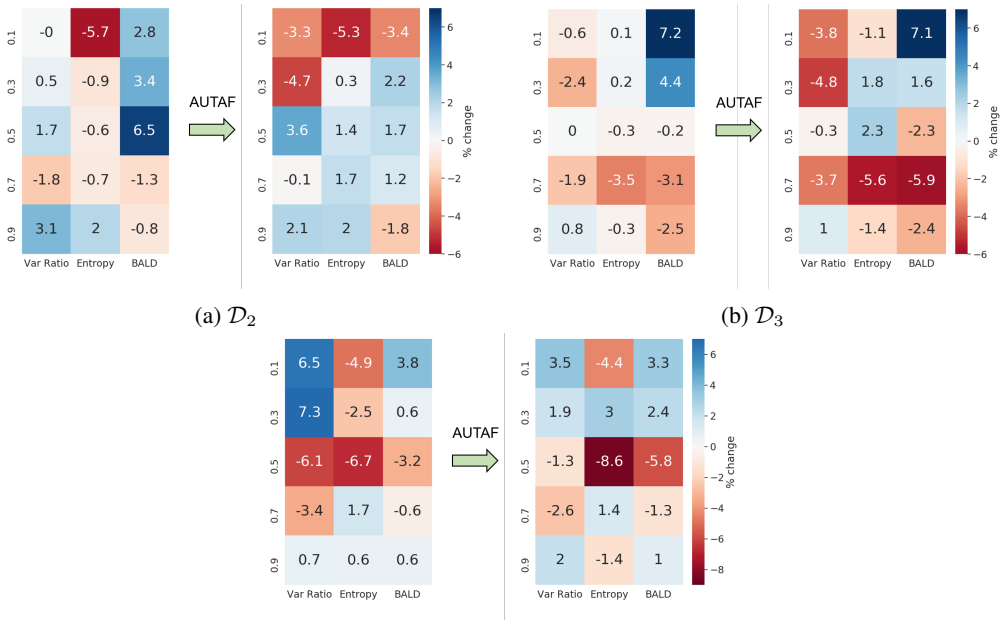

(a) $\mathcal{D}_2$ (b) $\mathcal{D}_3$

(c) $\mathcal{D}_4$

Figure 13: Mean percent change in test AUC when comparing MCP with static and tracked acquisition functions to MCD with their static counterparts on **(a)** $\mathcal{D}_2$ and **(b)** $\mathcal{D}_3$ and **(c)** $\mathcal{D}_4$. We show results for Var Ratio, Entropy, and BALD, at all fractions, $\beta \in [0.1, 0.3, 0.5, 0.7, 0.9]$.

L DEGREE OF DEPENDENCE OF SOQAL ON ORACLE

A naive argument could claim that SoQal's superiority is simply due to high oracle dependence. To test this hypothesis, we set out to quantify SoQal's dependence on an oracle using the oracle ask-rate: the proportion of all instances acquired whose labels are requested from an oracle. In Fig. 14a, we illustrate this oracle ask-rate for different label noise scenarios.

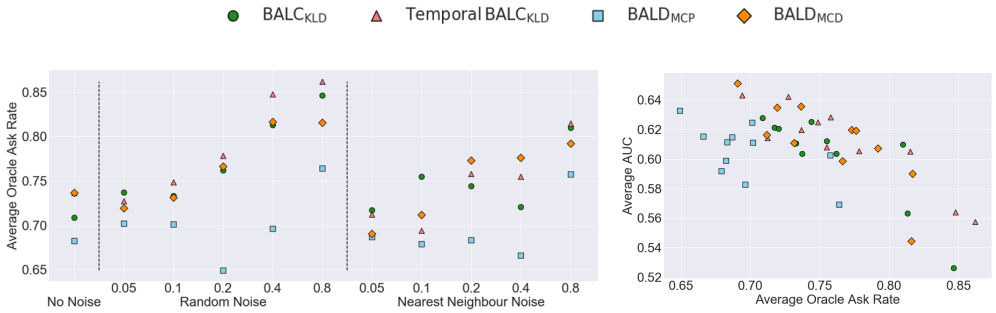

(a) Oracle ask-rate for different label noise scenarios

(b) Correlation between oracle ask-rate and generalization performance

Figure 14: (a) SoQal's average oracle ask-rate and (b) correlation between oracle ask-rate and average test AUC. Results are averaged across five seeds and all datasets, $\mathcal{D}_1 - \mathcal{D}_5$, and are shown for each acquisition function and label noise scenario.

The oracle ask-rate varies based on the acquisition function used. In Fig. 14a, we show that with 20% random noise, BALD$_{MCP}$ requests labels 65% of the time whereas the remaining acquisition functions do so approximately 77% of the time. We hypothesize that this variability in the oracle ask-rate is due to the variability in the difficulty of the instances acquired by the acquisition functions. In other words, decreased dependence by BALD$_{MCP}$ could be indicative of the acquisition of instances that are relatively farther away from the hyperplane. Thus, they are easier to classify and require less oracle guidance.

In the presence of label noise, decreased oracle dependence is actually associated with improved generalization performance. In Fig. 14b, this is shown by the negative correlation between the oracle ask-rate and the test AUC. Networks are requesting fewer labels and are performing better. Such a finding dispels the original claim and reaffirms the conclusion that SoQal knows *when* to request a label from an oracle.

M EFFECT OF DATA AVAILABILITY ON ORACLE ASK-RATE

As we performed all experiments on small, labelled datasets, we wanted to investigate the role of data availability on the amount of independence an algorithm can withstand. We hypothesize that access to large, labelled datasets would allow SoQal to decrease its overall dependence on an oracle while maintaining its generalization performance. In Table 12, we illustrate the effect of increasing the amount of labelled training data N-Fold, where $N = [3, 5, 7, 9]$, on the oracle ask-rate (OAR) and the generalization performance of a network.

Increasing the amount of labelled training data can drastically decrease oracle dependence *without* significantly affecting generalization performance. In Table 12, we show that a 5-fold increase in sample-size results in $\mathrm{OAR} = 100\% \rightarrow 59\%$, a 41% reduction in dependence while maintaining the test $\mathrm{AUC} \approx 0.59$. In other words, 41% of a physician's time can be reliably saved.

Table 12: Mean test AUC and oracle ask rate of a 100% oracle strategy and SoQal in response to more labelled training data. Results are shown for $\mathcal{D}_4$ and $\mathrm{BALD}_{\mathrm{MCD}}$ at $S = 0.15$ across five seeds. Original represents the small sample size used for all previous experiments.

Oracle Questioning Method	100% Oracle	SoQal				
Sample Size Factor	Original	Original	3-Fold	5-Fold	7-Fold	9-Fold
Average OAR %	100	48	56	59	68	67
AUC	0.585	0.468	0.507	0.594	0.659	0.657

N CONTROLLING ORACLE DEPENDENCE VIA HELLINGER THRESHOLD, S

In this section, we set out to investigate the degree to which the Hellinger threshold, S, acts as a knob that controls the oracle ask-rate (OAR). We expect this behaviour to arise from our design that when $\mathcal{D}_H < S$, all label requests are sent to the oracle. In Table 13, we show how different values of S affect the oracle ask-rate and the test AUC.

There exists a positive relationship between S and the oracle ask-rate. As $S = 0.100 \rightarrow 0.400$, the $\text{OAR} = 86\% \rightarrow 100\%$. In the presence of a noise-free oracle, we would expect this increased dependence to be associated with improved generalization performance. We observe such behaviour as $\text{OAR} = 86\% \rightarrow 94\%$ and $\text{AUC} = 0.716 \rightarrow 0.768$. However, increased dependence beyond this point is a detriment to performance. This finding reaffirms our previous hypothesis that the original labels in the dataset may be noisy. Therefore, a sub-100% OAR scenario in which these particular noisy labels are not requested from the oracle would be advantageous.

Table 13: Mean test AUC of SoQal and oracle ask rate in response to various threshold values, S. Results are shown for $\mathcal{D}_3$ and BALD_{MCD} across five seeds. Experiments are performed with a noise-free oracle.

Threshold, S	0.100	0.125	0.150	0.175	0.200	0.300	0.400
Average OAR %	86	85	89	90	94	100	100
AUC	0.716	0.744	0.721	0.753	0.768	0.743	0.755

O PERFORMANCE OF ORACLE SELECTION STRATEGIES WITH NOISY ORACLE

Over-reliance on an oracle could be detrimental for an active learning algorithm if that oracle is unable to label instances accurately. In the case of physicians, this inability could arise due to poor training, fatigue, or the difficulty of a particular case being diagnosed. We simulate these scenarios by injecting label noise of various magnitude into the datasets. In this section, we illustrate the performance of three oracle selection strategies, SoQal, Epsilon Greedy, and Entropy Response, in response to label noise. The results are shown for random and nearest neighbour noise in Secs. O.1 and O.2, respectively.

O.1 LABEL NOISE - RANDOM

Although random noise can be considered an extreme case, it is nonetheless plausible in certain scenarios where labellers are poorly trained or the task at hand is too difficult. In this section, we illustrate, in Tables 14a - 14c, the degree to which the test AUC is affected by the introduction of random label noise during the active learning procedure.

As expected, extreme levels of noise negatively affect performance. For instance, this can be seen in Table 14a at $\mathcal{D}_2$ using BALD_{MCD} where increasing the level of random noise from $5\% \rightarrow 80\%$ leads to a reduction of $\text{AUC} = 0.679 \rightarrow 0.556$. Across most noise levels, SoQal continues to outperform Epsilon Greedy and Entropy Response. This finding is consistent with that presented in the main manuscript and illustrates the relative robustness of SoQal to label noise.

Table 14: Mean test AUC of oracle questioning strategies as a function of increasing levels of *random* label noise by the oracle. Results are shown for datasets $\mathcal{D}_1 - \mathcal{D}_5$ and all acquisition functions. Mean and standard deviation values are shown across five seeds.

(a) SoQal

Dataset	Ac. Function α	Random Noise Level				
		0.05	0.10	0.20	0.40	0.80
$\mathcal{D}_1$	BALD_{MCD}	0.595 ± 0.053	0.554 ± 0.028	0.558 ± 0.042	0.600 ± 0.029	0.511 ± 0.055
	BALD_{MCP}	0.659 ± 0.014	0.650 ± 0.027	0.636 ± 0.029	0.549 ± 0.058	0.528 ± 0.029
	BALC_{KLD}	0.564 ± 0.058	0.570 ± 0.045	0.562 ± 0.067	0.498 ± 0.038	0.477 ± 0.011
	Temporal BALC_{KLD}	0.634 ± 0.026	0.597 ± 0.035	0.611 ± 0.040	0.494 ± 0.034	0.490 ± 0.026
$\mathcal{D}_2$	BALD_{MCD}	0.679 ± 0.017	0.659 ± 0.042	0.646 ± 0.044	0.602 ± 0.047	0.556 ± 0.065
	BALD_{MCP}	0.643 ± 0.020	0.677 ± 0.053	0.637 ± 0.042	0.619 ± 0.033	0.602 ± 0.041
	BALC_{KLD}	0.652 ± 0.037	0.659 ± 0.056	0.649 ± 0.054	0.614 ± 0.016	0.522 ± 0.032
	Temporal BALC_{KLD}	0.655 ± 0.048	0.701 ± 0.029	0.628 ± 0.074	0.594 ± 0.041	0.581 ± 0.032
$\mathcal{D}_3$	BALD_{MCD}	0.750 ± 0.017	0.742 ± 0.031	0.718 ± 0.037	0.646 ± 0.023	0.584 ± 0.017
	BALD_{MCP}	0.724 ± 0.022	0.707 ± 0.021	0.682 ± 0.038	0.629 ± 0.029	0.537 ± 0.025
	BALC_{KLD}	0.724 ± 0.032	0.725 ± 0.028	0.702 ± 0.024	0.651 ± 0.046	0.564 ± 0.040
	Temporal BALC_{KLD}	0.725 ± 0.031	0.738 ± 0.013	0.705 ± 0.017	0.596 ± 0.071	0.546 ± 0.041
$\mathcal{D}_4$	BALD_{MCD}	0.506 ± 0.019	0.479 ± 0.022	0.496 ± 0.023	0.490 ± 0.010	0.518 ± 0.029
	BALD_{MCP}	0.499 ± 0.037	0.508 ± 0.022	0.523 ± 0.027	0.495 ± 0.023	0.503 ± 0.021
	BALC_{KLD}	0.491 ± 0.026	0.481 ± 0.023	0.496 ± 0.031	0.518 ± 0.012	0.525 ± 0.011
	Temporal BALC_{KLD}	0.522 ± 0.016	0.505 ± 0.027	0.501 ± 0.021	0.511 ± 0.025	0.515 ± 0.031

(b) Epsilon Greedy

Dataset	Ac. Function α	Random Noise Level 0.05	0.10	0.20	0.40	0.80
$\mathcal{D}_1$	$\mathrm{BALD}_{\mathrm{MCD}}$	0.496± 0.058	0.494 ± 0.029	0.476 ± 0.030	0.507 ± 0.044	0.501 ± 0.056
	$\mathrm{BALD}_{\mathrm{MCP}}$	0.557 ± 0.018	0.549 ± 0.036	0.508 ± 0.032	0.511 ± 0.033	0.497 ± 0.057
	$\mathrm{BALC}_{\mathrm{KLD}}$	0.517 ± 0.014	0.518 ± 0.035	0.504 ± 0.028	0.506 ± 0.034	0.498 ± 0.017
	Temporal $\mathrm{BALC}_{\mathrm{KLD}}$	0.525 ± 0.037	0.512 ± 0.040	0.501 ± 0.025	0.493 ± 0.019	0.497 ± 0.039
$\mathcal{D}_2$	$\mathrm{BALD}_{\mathrm{MCD}}$	0.600± 0.053	0.628 ± 0.053	0.589 ± 0.037	0.612 ± 0.022	0.555 ± 0.041
	$\mathrm{BALD}_{\mathrm{MCP}}$	0.629 ± 0.023	0.614 ± 0.048	0.536 ± 0.081	0.575 ± 0.029	0.588 ± 0.050
	$\mathrm{BALC}_{\mathrm{KLD}}$	0.619 ± 0.038	0.586 ± 0.054	0.629 ± 0.061	0.613 ± 0.045	0.582 ± 0.067
	Temporal $\mathrm{BALC}_{\mathrm{KLD}}$	0.630 ± 0.041	0.652 ± 0.029	0.579 ± 0.034	0.610 ± 0.036	0.564 ± 0.035
$\mathcal{D}_3$	$\mathrm{BALD}_{\mathrm{MCD}}$	0.663 ± 0.018	0.661 ± 0.011	0.632 ± 0.021	0.626± 0.012	0.588 ± 0.017
	$\mathrm{BALD}_{\mathrm{MCP}}$	0.671 ± 0.017	0.670 ± 0.016	0.639 ± 0.024	0.623 ± 0.019	0.574 ± 0.041
	$\mathrm{BALC}_{\mathrm{KLD}}$	0.665 ± 0.022	0.650 ± 0.014	0.664 ± 0.013	0.618 ± 0.034	0.595 ± 0.031
	Temporal $\mathrm{BALC}_{\mathrm{KLD}}$	0.661 ± 0.012	0.651 ± 0.018	0.651 ± 0.016	0.629 ± 0.019	0.612 ± 0.049
$\mathcal{D}_4$	$\mathrm{BALD}_{\mathrm{MCD}}$	0.473 ± 0.030	0.480 ± 0.033	0.469 ± 0.024	0.468± 0.018	0.493 ± 0.015
	$\mathrm{BALD}_{\mathrm{MCP}}$	0.508 ± 0.016	0.495 ± 0.019	0.498 ± 0.043	0.494 ± 0.032	0.497 ± 0.015
	$\mathrm{BALC}_{\mathrm{KLD}}$	0.492 ± 0.026	0.496 ± 0.021	0.481 ± 0.025	0.491 ± 0.020	0.498 ± 0.021
	Temporal $\mathrm{BALC}_{\mathrm{KLD}}$	0.514 ± 0.017	0.528 ± 0.017	0.500 ± 0.008	0.498 ± 0.033	0.504 ± 0.037

(c) Entropy Response

Dataset	Ac. Function α	Random Noise Level 0.05	0.10	0.20	0.40	0.80
$\mathcal{D}_1$	$\mathrm{BALD}_{\mathrm{MCD}}$	0.495 ± 0.038	0.497 ± 0.057	0.498 ± 0.057	0.486 ± 0.044	0.512 ± 0.057
	$\mathrm{BALD}_{\mathrm{MCP}}$	0.534 ± 0.018	0.584 ± 0.073	0.565 ± 0.033	0.619 ± 0.022	0.518 ± 0.028
	$\mathrm{BALC}_{\mathrm{KLD}}$	0.535 ± 0.038	0.521 ± 0.042	0.514 ± 0.053	0.511 ± 0.027	0.525 ± 0.037
	Temporal $\mathrm{BALC}_{\mathrm{KLD}}$	0.526 ± 0.040	0.538 ± 0.036	0.504 ± 0.028	0.501 ± 0.036	0.500 ± 0.004
$\mathcal{D}_2$	$\mathrm{BALD}_{\mathrm{MCD}}$	0.587 ± 0.044	0.564 ± 0.058	0.586 ± 0.047	0.613 ± 0.083	0.551 ± 0.031
	$\mathrm{BALD}_{\mathrm{MCP}}$	0.624 ± 0.044	0.598 ± 0.057	0.573 ± 0.053	0.560 ± 0.081	0.530 ± 0.015
	$\mathrm{BALC}_{\mathrm{KLD}}$	0.616 ± 0.043	0.653 ± 0.049	0.624 ± 0.051	0.565 ± 0.055	0.579 ± 0.019
	Temporal $\mathrm{BALC}_{\mathrm{KLD}}$	0.635 ± 0.045	0.603 ± 0.050	0.590 ± 0.042	0.602 ± 0.046	0.579 ± 0.041
$\mathcal{D}_3$	$\mathrm{BALD}_{\mathrm{MCD}}$	0.592 ± 0.015	0.604 ± 0.017	0.603 ± 0.016	0.603 ± 0.016	0.605 ± 0.018
	$\mathrm{BALD}_{\mathrm{MCP}}$	0.694 ± 0.047	0.730 ± 0.029	0.666 ± 0.034	0.639 ± 0.031	0.599 ± 0.035
	$\mathrm{BALC}_{\mathrm{KLD}}$	0.631 ± 0.006	0.631 ± 0.009	0.622 ± 0.011	0.631 ± 0.025	0.564 ± 0.046
	Temporal $\mathrm{BALC}_{\mathrm{KLD}}$	0.602 ± 0.011	0.622 ± 0.018	0.630 ± 0.014	0.618 ± 0.040	0.565 ± 0.050
$\mathcal{D}_4$	$\mathrm{BALD}_{\mathrm{MCD}}$	0.472 ± 0.029	0.472 ± 0.030	0.486 ± 0.008	0.476 ± 0.038	0.481 ± 0.038
	$\mathrm{BALD}_{\mathrm{MCP}}$	0.511 ± 0.021	0.510 ± 0.023	0.525 ± 0.033	0.498 ± 0.041	0.497 ± 0.017
	$\mathrm{BALC}_{\mathrm{KLD}}$	0.468 ± 0.022	0.472 ± 0.029	0.477 ± 0.029	0.483 ± 0.018	0.475 ± 0.032
	Temporal $\mathrm{BALC}_{\mathrm{KLD}}$	0.482 ± 0.023	0.491 ± 0.013	0.490 ± 0.021	0.487 ± 0.031	0.515 ± 0.022

O.2 LABEL NOISE - NEAREST NEIGHBOUR

Nearest neighbour noise is more realistic than that which is random as it may simulate uncertainty in diagnoses made by physicians. In this section, we illustrate, in Tables 15a - 15c, the degree to which the test AUC is affected by the introduction of nearest neighbour label noise during the active learning procedure.

As expected, extreme levels of noise negatively affect performance. For instance, this can be seen in Table 15a at $\mathcal{D}_3$ using BALD_{MCD} where increasing the level of nearest neighbour noise from $5\% \rightarrow 80\%$ leads to a reduction of the $\text{AUC} = 0.744 \rightarrow 0.694$. SoQal continues to outperform Epsilon Greedy and Entropy Response across most of the noise levels. Building on the previous example, with 80% nearest neighbour noise, SoQal achieves an $\text{AUC} = 0.694$ whereas Epsilon Greedy and Entropy Response achieve an $\text{AUC} = 0.632$ and 0.587, respectively. Such a finding is similar to that arrived at with Random Noise and implies that SoQal is relatively more robust to noisy oracles than these other methods.

Table 15: Mean test AUC of oracle questioning strategies as a function of increasing levels of *nearest neighbour* label noise by the oracle. Results are shown for datasets $\mathcal{D}_1 - \mathcal{D}_5$ and all acquisition functions. Mean and standard deviation values are shown across five seeds.

(a) SoQal

Dataset	Ac. Function α	Nearest Neighbour Noise Level				
		0.05	0.10	0.20	0.40	0.80
$\mathcal{D}_1$	BALD_{MCD}	0.614 ± 0.043	0.571 ± 0.037	0.618 ± 0.015	0.557 ± 0.042	0.540 ± 0.052
	BALD_{MCP}	0.633 ± 0.011	0.617 ± 0.095	0.641 ± 0.023	0.632 ± 0.026	0.591 ± 0.047
	BALC_{KLD}	0.628 ± 0.049	0.586 ± 0.032	0.616 ± 0.024	0.604 ± 0.022	0.558 ± 0.069
	Temporal BALC_{KLD}	0.557 ± 0.045	0.647 ± 0.060	0.620 ± 0.036	0.625 ± 0.038	0.577 ± 0.039
$\mathcal{D}_2$	BALD_{MCD}	0.694 ± 0.022	0.631 ± 0.020	0.682 ± 0.036	0.658 ± 0.038	0.647 ± 0.039
	BALD_{MCP}	0.605 ± 0.054	0.660 ± 0.067	0.656 ± 0.029	0.618 ± 0.058	0.605 ± 0.081
	BALC_{KLD}	0.655 ± 0.015	0.660 ± 0.037	0.671 ± 0.078	0.649 ± 0.024	0.678 ± 0.023
	Temporal BALC_{KLD}	0.702 ± 0.044	0.654 ± 0.024	0.686 ± 0.038	0.638 ± 0.042	0.631 ± 0.020
$\mathcal{D}_3$	BALD_{MCD}	0.744 ± 0.023	0.745 ± 0.021	0.709 ± 0.028	0.700 ± 0.026	0.694 ± 0.014
	BALD_{MCP}	0.706 ± 0.029	0.736 ± 0.036	0.727 ± 0.023	0.712 ± 0.018	0.682 ± 0.017
	BALC_{KLD}	0.718 ± 0.029	0.729 ± 0.028	0.735 ± 0.021	0.680 ± 0.050	0.688 ± 0.009
	Temporal BALC_{KLD}	0.727 ± 0.033	0.725 ± 0.033	0.724 ± 0.018	0.700 ± 0.022	0.645 ± 0.062
$\mathcal{D}_4$	BALD_{MCD}	0.517 ± 0.034	0.477 ± 0.027	0.493 ± 0.034	0.498 ± 0.036	0.459 ± 0.035
	BALD_{MCP}	0.492 ± 0.027	0.491 ± 0.027	0.502 ± 0.036	0.532 ± 0.040	0.507 ± 0.042
	BALC_{KLD}	0.494 ± 0.024	0.494 ± 0.016	0.504 ± 0.026	0.506 ± 0.031	0.503 ± 0.021
	Temporal BALC_{KLD}	0.504 ± 0.018	0.515 ± 0.013	0.529 ± 0.027	0.507 ± 0.014	0.508 ± 0.026

(b) Epsilon Greedy

Dataset	Ac. Function α	Nearest Neighbour Noise Level 0.05	0.10	0.20	0.40	0.80
$\mathcal{D}_1$	$\mathrm{BALD}_{\mathrm{MCD}}$	0.503 ± 0.040	0.480 ± 0.023	0.514 ± 0.050	0.481 ± 0.038	0.456 ± 0.031
	$\mathrm{BALD}_{\mathrm{MCP}}$	0.501 ± 0.014	0.508 ± 0.036	0.522 ± 0.052	0.482 ± 0.023	0.496 ± 0.041
	$\mathrm{BALC}_{\mathrm{KLD}}$	0.541 ± 0.035	0.503 ± 0.033	0.486 ± 0.047	0.500 ± 0.041	0.473 ± 0.026
	Temporal $\mathrm{BALC}_{\mathrm{KLD}}$	0.516 ± 0.024	0.523 ± 0.044	0.495 ± 0.046	0.491 ± 0.013	0.483 ± 0.041
$\mathcal{D}_2$	$\mathrm{BALD}_{\mathrm{MCD}}$	0.584 ± 0.066	0.610 ± 0.042	0.597 ± 0.036	0.616 ± 0.054	0.593 ± 0.054
	$\mathrm{BALD}_{\mathrm{MCP}}$	0.565 ± 0.031	0.589 ± 0.075	0.616 ± 0.059	0.605 ± 0.047	0.586 ± 0.047
	$\mathrm{BALC}_{\mathrm{KLD}}$	0.608 ± 0.031	0.607 ± 0.040	0.590 ± 0.055	0.538 ± 0.037	0.585 ± 0.053
	Temporal $\mathrm{BALC}_{\mathrm{KLD}}$	0.647 ± 0.044	0.591 ± 0.033	0.640 ± 0.044	0.576 ± 0.031	0.589 ± 0.030
$\mathcal{D}_3$	$\mathrm{BALD}_{\mathrm{MCD}}$	0.656 ± 0.021	0.655 ± 0.014	0.665 ± 0.010	0.643 ± 0.021	0.632 ± 0.010
	$\mathrm{BALD}_{\mathrm{MCP}}$	0.660 ± 0.022	0.657 ± 0.023	0.659 ± 0.003	0.664 ± 0.023	0.634 ± 0.013
	$\mathrm{BALC}_{\mathrm{KLD}}$	0.608 ± 0.031	0.607 ± 0.040	0.590 ± 0.055	0.538 ± 0.037	0.585 ± 0.053
	Temporal $\mathrm{BALC}_{\mathrm{KLD}}$	0.644 ± 0.016	0.651 ± 0.011	0.658 ± 0.013	0.634 ± 0.016	0.627 ± 0.014
$\mathcal{D}_4$	$\mathrm{BALD}_{\mathrm{MCD}}$	0.438 ± 0.014	0.457 ± 0.022	0.442 ± 0.018	0.456 ± 0.028	0.428 ± 0.024
	$\mathrm{BALD}_{\mathrm{MCP}}$	0.489 ± 0.018	0.489 ± 0.021	0.474 ± 0.023	0.485 ± 0.019	0.486 ± 0.015
	$\mathrm{BALC}_{\mathrm{KLD}}$	0.485 ± 0.029	0.487 ± 0.019	0.495 ± 0.023	0.488 ± 0.028	0.481 ± 0.021
	Temporal $\mathrm{BALC}_{\mathrm{KLD}}$	0.486 ± 0.018	0.500 ± 0.029	0.486 ± 0.027	0.468 ± 0.017	0.487 ± 0.028

(c) Entropy Response

Dataset	Ac. Function α	Nearest Neighbour Noise Level 0.05	0.10	0.20	0.40	0.80
$\mathcal{D}_1$	$\mathrm{BALD}_{\mathrm{MCD}}$	0.494 ± 0.037	0.474 ± 0.027	0.492 ± 0.051	0.482 ± 0.033	0.444 ± 0.006
	$\mathrm{BALD}_{\mathrm{MCP}}$	0.511 ± 0.019	0.562 ± 0.052	0.509 ± 0.042	0.572 ± 0.060	0.495 ± 0.041
	$\mathrm{BALC}_{\mathrm{KLD}}$	0.513 ± 0.020	0.517 ± 0.035	0.504 ± 0.034	0.498 ± 0.023	0.487 ± 0.023
	Temporal $\mathrm{BALC}_{\mathrm{KLD}}$	0.500 ± 0.043	0.540 ± 0.025	0.503 ± 0.043	0.516 ± 0.024	0.490 ± 0.024
$\mathcal{D}_2$	$\mathrm{BALD}_{\mathrm{MCD}}$	0.585 ± 0.045	0.630 ± 0.056	0.600 ± 0.045	0.585 ± 0.046	0.586 ± 0.063
	$\mathrm{BALD}_{\mathrm{MCP}}$	0.633 ± 0.060	0.626 ± 0.064	0.618 ± 0.055	0.647 ± 0.077	0.619 ± 0.055
	$\mathrm{BALC}_{\mathrm{KLD}}$	0.605 ± 0.049	0.572 ± 0.032	0.630 ± 0.081	0.581 ± 0.031	0.589 ± 0.061
	Temporal $\mathrm{BALC}_{\mathrm{KLD}}$	0.625 ± 0.030	0.599 ± 0.024	0.613 ± 0.050	0.614 ± 0.052	0.606 ± 0.054
$\mathcal{D}_3$	$\mathrm{BALD}_{\mathrm{MCD}}$	0.604 ± 0.017	0.589 ± 0.013	0.592 ± 0.014	0.592 ± 0.014	0.587 ± 0.012
	$\mathrm{BALD}_{\mathrm{MCP}}$	0.636 ± 0.030	0.635 ± 0.030	0.640 ± 0.040	0.634 ± 0.039	0.623 ± 0.032
	$\mathrm{BALC}_{\mathrm{KLD}}$	0.632 ± 0.008	0.633 ± 0.008	0.630 ± 0.005	0.629 ± 0.004	0.625 ± 0.008
	Temporal $\mathrm{BALC}_{\mathrm{KLD}}$	0.631 ± 0.013	0.630 ± 0.013	0.637 ± 0.013	0.630 ± 0.014	0.629 ± 0.009
$\mathcal{D}_4$	$\mathrm{BALD}_{\mathrm{MCD}}$	0.475 ± 0.035	0.493 ± 0.025	0.471 ± 0.031	0.468 ± 0.027	0.481 ± 0.035
	$\mathrm{BALD}_{\mathrm{MCP}}$	0.508 ± 0.024	0.512 ± 0.020	0.513 ± 0.019	0.499 ± 0.012	0.492 ± 0.016
	$\mathrm{BALC}_{\mathrm{KLD}}$	0.483 ± 0.031	0.476 ± 0.033	0.473 ± 0.026	0.479 ± 0.021	0.479 ± 0.032
	Temporal $\mathrm{BALC}_{\mathrm{KLD}}$	0.490 ± 0.012	0.497 ± 0.030	0.466 ± 0.013	0.485 ± 0.016	0.500 ± 0.013

P EFFECT OF NUMBER OF MONTE CARLO SAMPLES, T, ON PERFORMANCE

The number of MC samples, T, within an AL framework can be associated with an improved approximation of the version space. This, in turn, should lead to improved AL results. To quantify the effect of the number of MC samples on performance, we illustrate in Fig. 15, the validation AUC for experiments conducted with $T = (5, 20, 40, 100)$. We show that there does not exist a simple proportional relationship between the number of MC samples and performance. This can be seen by the relatively strong generalization performance of models when $T = 100$ in Figs. 15c, 15h, and 15i and poorer performance when $T = 100$. This suggests that our family of methods can perform well without being computationally expensive.

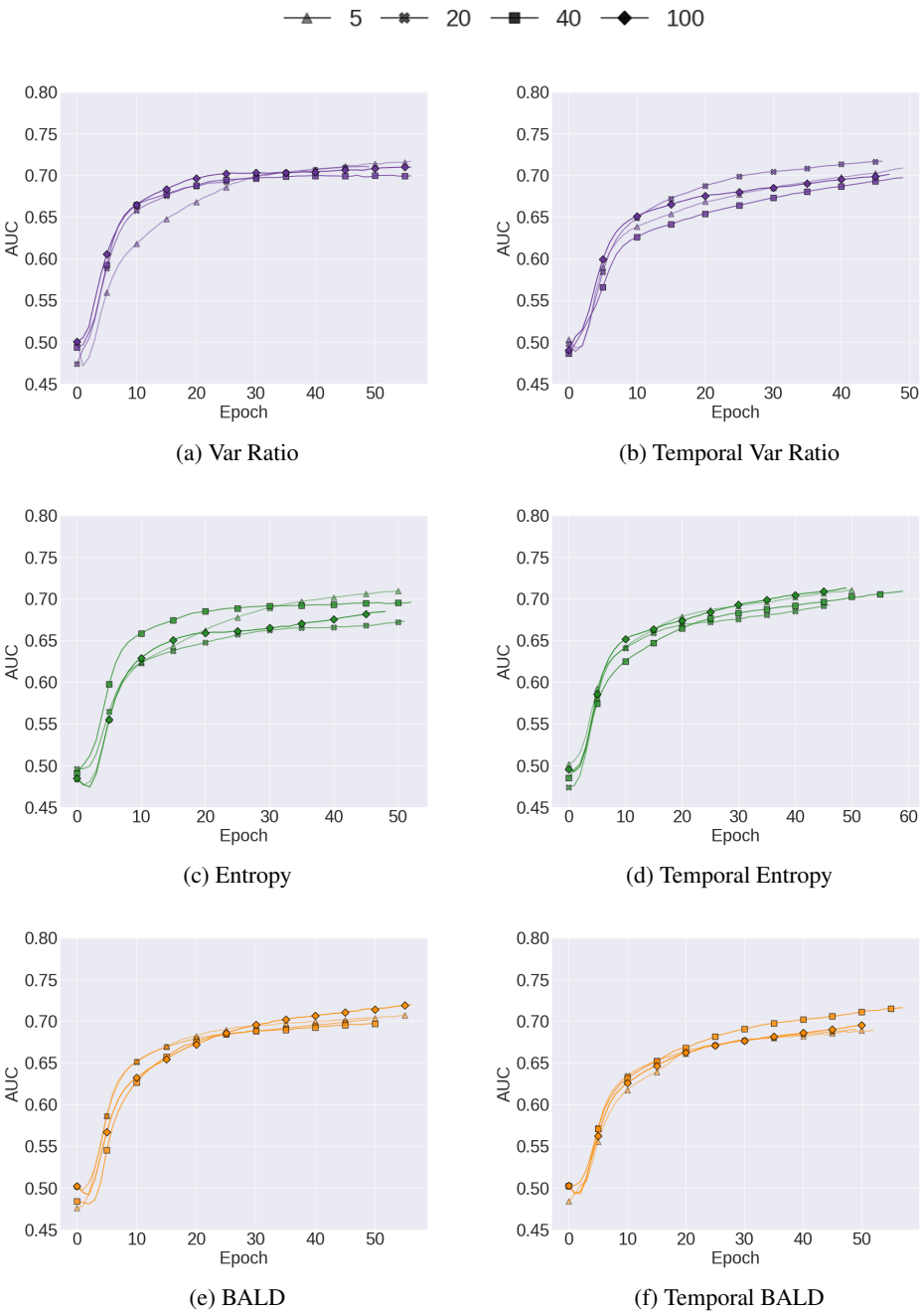

(a) Var Ratio

(b) Temporal Var Ratio

(c) Entropy

(d) Temporal Entropy

(e) BALD

(f) Temporal BALD

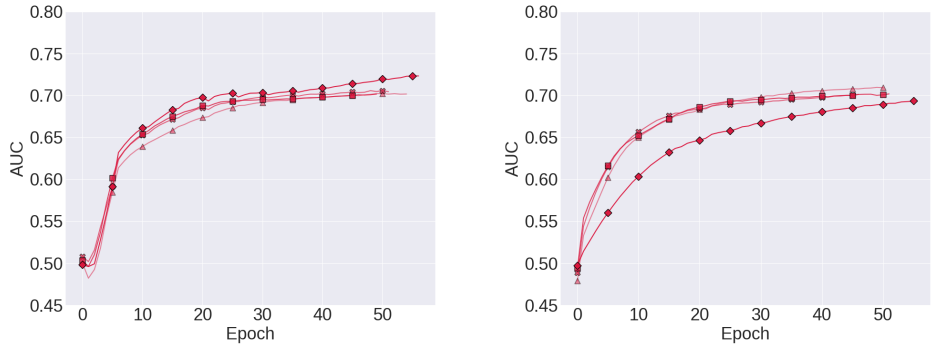

(g) BALC_{KLD} (h) Temporal BALC_{KLD}

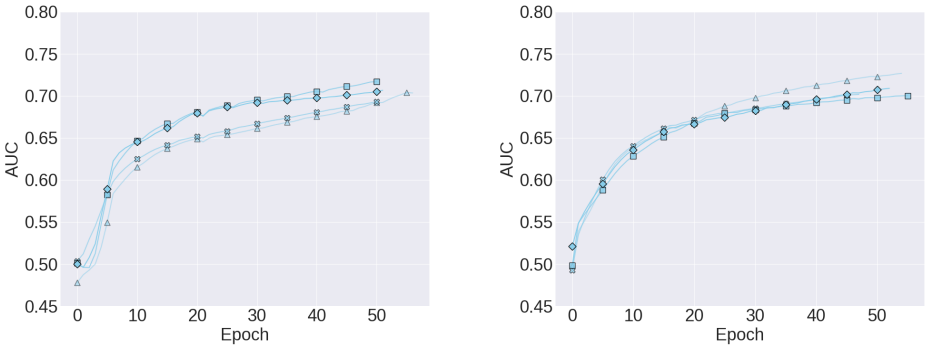

(i) BALC_{JSD} (j) Temporal BALC_{JSD}

Figure 15: Mean validation AUC as a function of number of Monte Carlo samples T for the different acquisition functions using the MCP method. The acquisition percentage and acquisition epochs were fixed at $b = 2\%$ and $\tau = 5$, respectively. These experiments are performed on $\mathcal{D}_2$ at a fraction of $\beta = 0.5$. Results are averaged across 5 seeds.

Q EFFECT OF ACQUISITION PERCENTAGE, b, ON PERFORMANCE

The number of unlabelled instances acquired during the AL procedure can have a strong effect on the generalization performance of networks. We investigate the effect of this on our family of methods and illustrate the results in Fig. 16 when conducting experiments for $b = (1\%, 2\%, 5\%, 20\%)$. Contrary to expectations that more acquisition is better, we show that acquiring large amounts of data is actually detrimental. This can be seen by the poorer performance attributed to $b = 20\%$ in, for instance, Figs. 16b, 16f, and 16g. We hypothesize that this is due to larger magnitude 1) distribution shifts and 2) label noise brought about by the absence of an oracle.

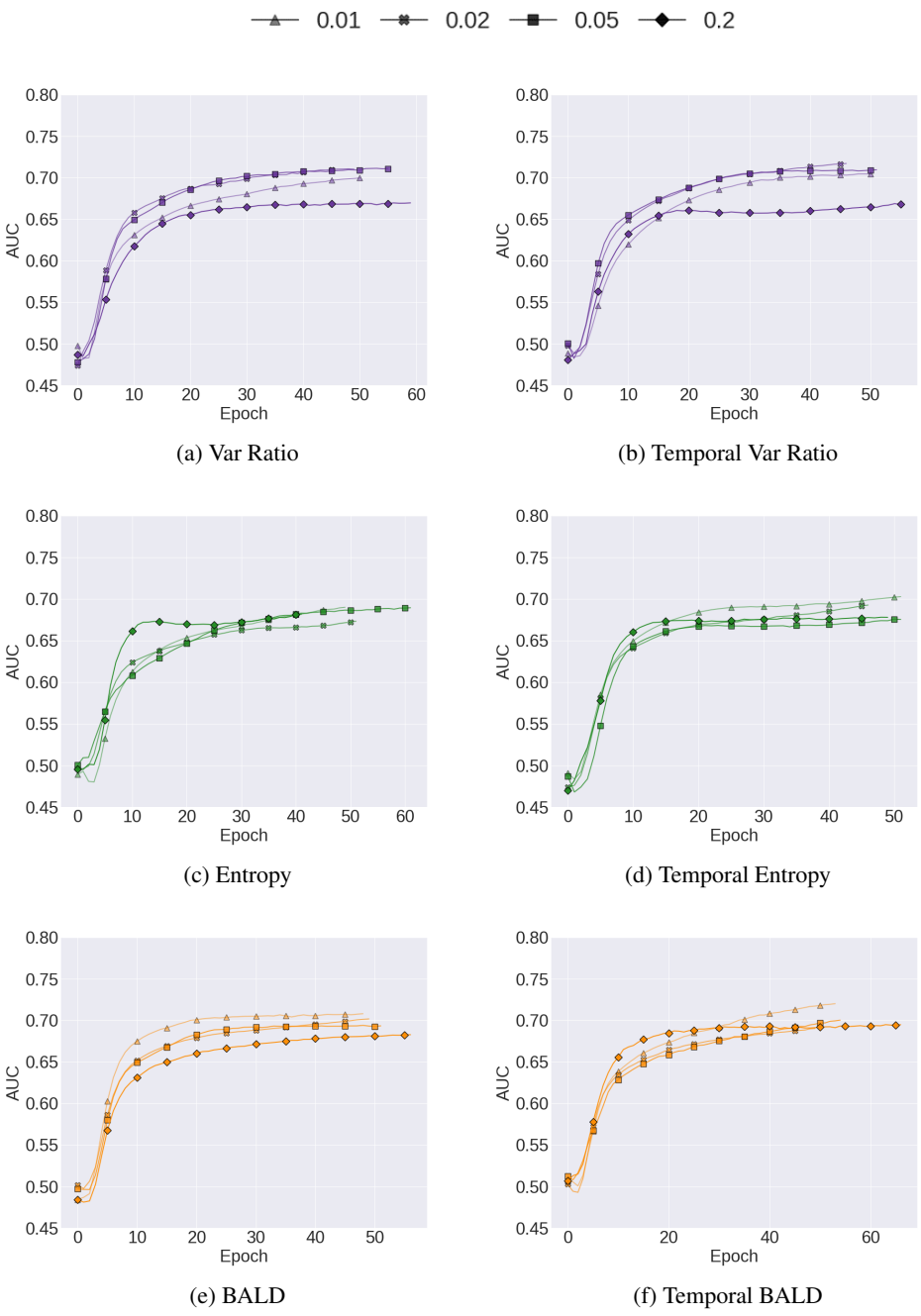

(a) Var Ratio

(b) Temporal Var Ratio

(c) Entropy

(d) Temporal Entropy

(e) BALD

(f) Temporal BALD

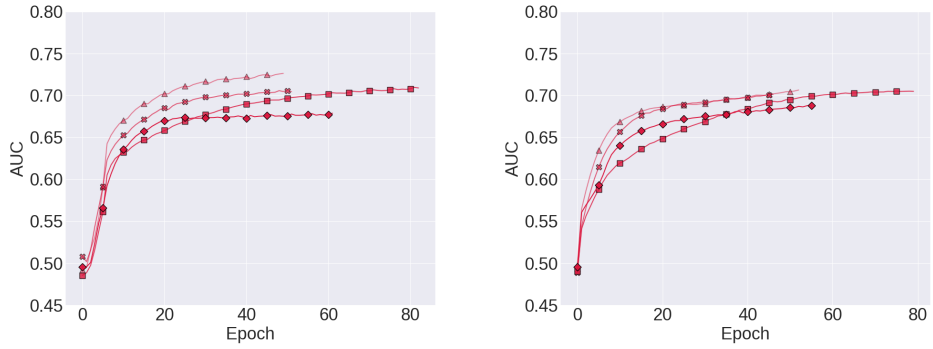

(g) BALC_{KLD}

(h) Temporal BALC_{KLD}

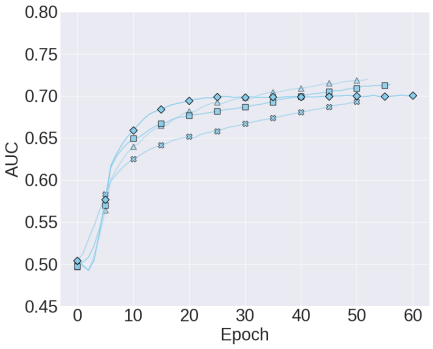

(i) BALC_{JSD}

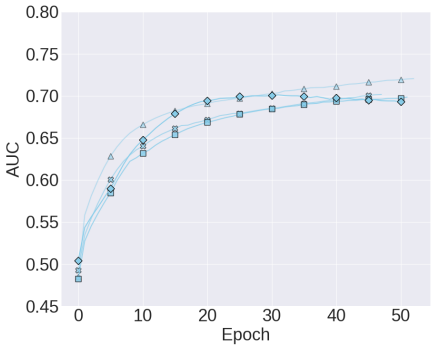

(j) Temporal BALC_{JSD}

Figure 16: Mean AUC of the validation set as a function of acquisition percentage b for the different acquisition functions using the MCP method. These experiments are performed on $\mathcal{D}_2$ at a fraction $\beta = 0.5$. MC samples and acquisition epochs were fixed at $T = 20$ and $\tau = 5$, respectively. Results are averaged across 5 seeds.

R EFFECT OF ACQUISITION EPOCHS, τ, ON PERFORMANCE

As outlined in the main manuscript, the control vs. shock trade-off must be balanced to ensure good generalization performance of an AL procedure. Acquiring instances too early and frequently can lead to instabilities in the training procedure. Conversely, inadequate sampling of unlabelled instances starves the network of much needed data. To quantify this trade-off, we illustrate in Fig. 17, the performance of our family of methods when $\tau = (5, 10, 15, 20)$. Although one value that guarantees best performance for all experiments does not exist, $\tau = 10$ or $\tau = 15$ seem to outperform the others, on average.

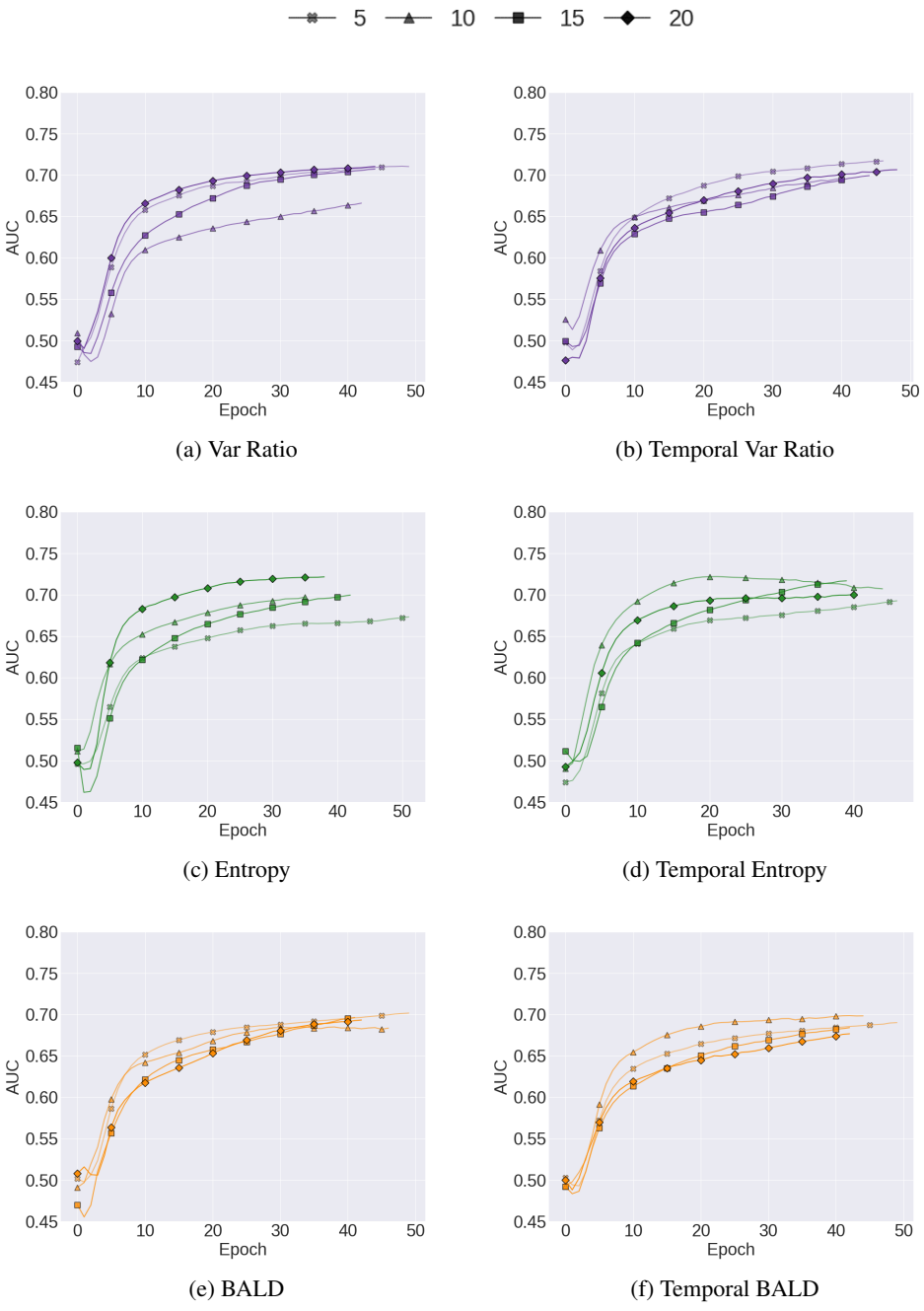

(a) Var Ratio

(b) Temporal Var Ratio

(c) Entropy

(d) Temporal Entropy

(e) BALD

(f) Temporal BALD

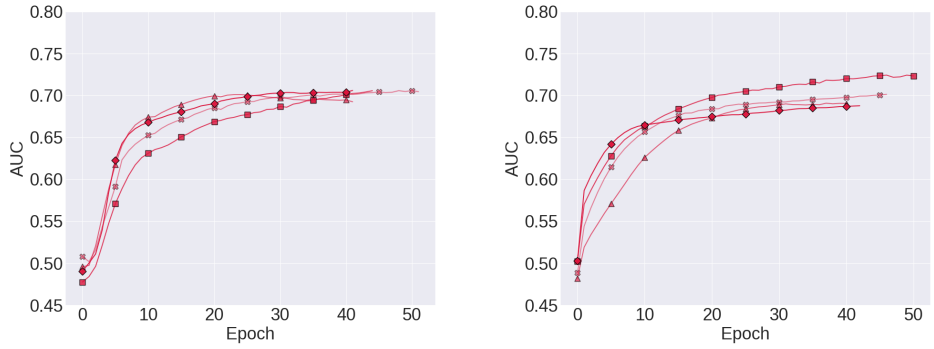

(g) BALC_{KLD} (h) Temporal BALC_{KLD}

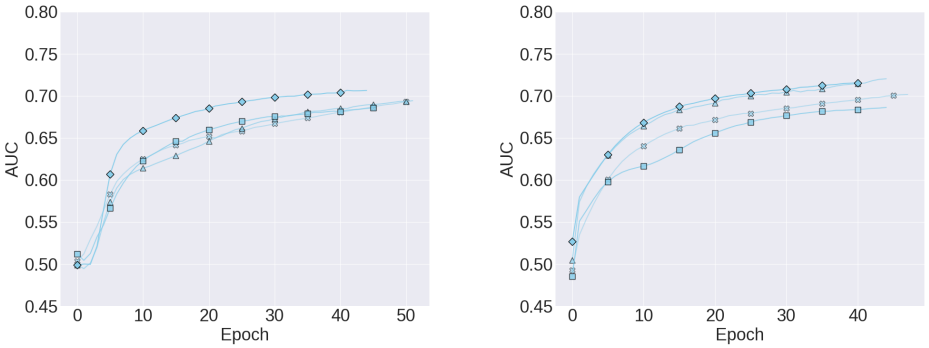

(i) BALC_{JSD} (j) Temporal BALC_{JSD}

Figure 17: Mean AUC of the validation set as a function of acquisition epochs τ for the different acquisition functions using the MCP method. MC samples and the acquistion percentage were fixed at $T = 20$ and $b = 2\%$, respectively. These experiments are performed on $\mathcal{D}_2$ at a fraction $\beta = 0.5$. Results are averaged across 5 seeds.